Hindawi Publishing Corporation
Advances in Fuzzy Systems
Volume 2013, Article ID 164853, 16 pages
http://dx.doi.org/10.1155/2013/164853

Research Article

Analysis of Adaptive Fuzzy Technique for Multiple Crack Diagnosis of Faulty Beam Using Vibration Signatures

Amiya Kumar Dash

Department of Mechanical Engineering, SiKsha 'O' Anusandhan University, Bhubaneswar, Orissa 751030, India

Correspondence should be addressed to Amiya Kumar Dash; dash.amiya@gmail.com

Received 22 April 2012; Accepted 7 December 2012

Academic Editor: Ashu M. G. Solo

Copyright © 2013 Amiya Kumar Dash. This is an open access article distributed under the Creative Commons Attribution License, which permits unrestricted use, distribution, and reproduction in any medium, provided the original work is properly cited.

This paper discusses the multicrack detection of structure using fuzzy Gaussian technique. The vibration parameters derived from the numerical methods of the cracked cantilever beam are used to set several fuzzy rules for designing the fuzzy controller used to predict the crack location and depth. Relative crack locations and relative crack depths are the output parameters from the fuzzy inference system. The method proposed in the current analysis is used to evaluate the dynamic response of cracked cantilever beam. The results of the proposed method are in good agreement with the results obtained from the developed experimental setup.

1. Introduction

Beams are one of the most commonly used structural elements in numerous engineering applications and experience a wide variety of static and dynamic loads. Cracks may develop in beam-like structures due to such loads. Considering the crack as a significant form of such damage, its modeling is an important step in studying the behavior of damaged structures. As stated, beam type structures are being commonly used in steel construction and machinery industries. Studies based on structural health monitoring for crack detection deal with change in natural frequencies and mode shapes of the beam.

An analytical study has been performed by Yang et al. [1] on the free and forced vibration of inhomogeneous Euler-Bernoulli beams containing open edge cracks. Analytical solutions are obtained for cantilever, with different end conditions to evaluate the dynamic response of the beam due to the edge crack. Orhan [2] has performed a free and forced vibration analysis of a cracked beam in order to identify the cracks in a cantilever beam. Their study reveals that free vibration analysis provides more suitable information for the detection of cracks than the forced vibration analysis. Damage in a cracked structure has been analyzed using genetic algorithm technique by Vakil-Baghmisheh et al. [3]. For modeling the cracked-beam structure, an analytical model of a cracked cantilever beam has been utilized, and natural frequencies are obtained through numerical methods. A genetic algorithm is utilized to monitor the possible changes in the natural frequencies of the structure. Theoretical and experimental dynamic behaviors of different multibeams systems containing a transverse crack have been performed by Saavedra and Cuitio [4]. A new cracked stiffness matrix is deduced based on flexibility, and this can be used subsequently in the FEM analysis of crack systems. Bakhary et al. [5] used Artificial Neural Network (ANN) for damage detection. In his analysis, an ANN model is created by applying Rosenblueth's point estimate method verified by Monte Carlo simulation. The results have demonstrated that the statistical ANN approach gives more reliable identification of structural damage. Friswell et al. [6] have applied genetic algorithm to the problem of damage detection using vibration data. The objective is to identify the position of one or more damage sites in a structure and to estimate the extent of the damage. A comprehensive analysis of the stability of a cracked beam subjected to a follower compressive load is presented by Wang [7]. The vibration analysis on such cracked beam has been conducted to identify the critical

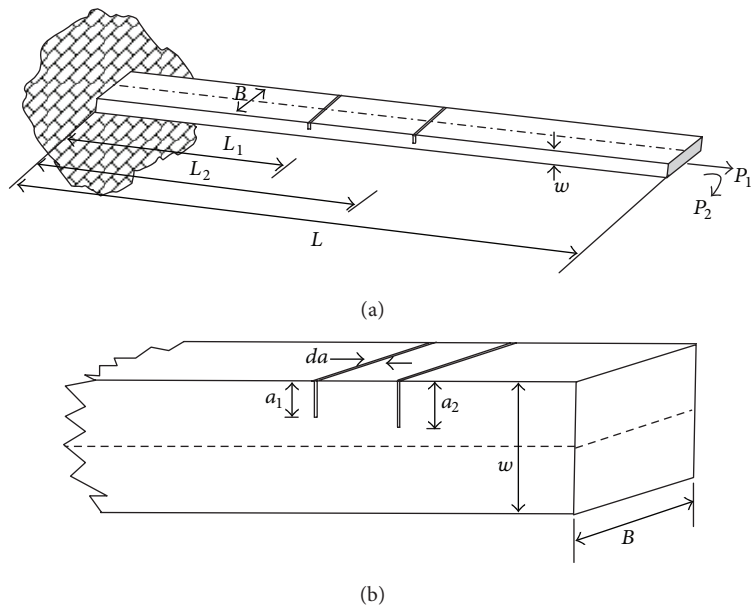

Figure 1: Geometry of beam. (a) Cantilever beam. (b) Cross-sectional view of the beam.

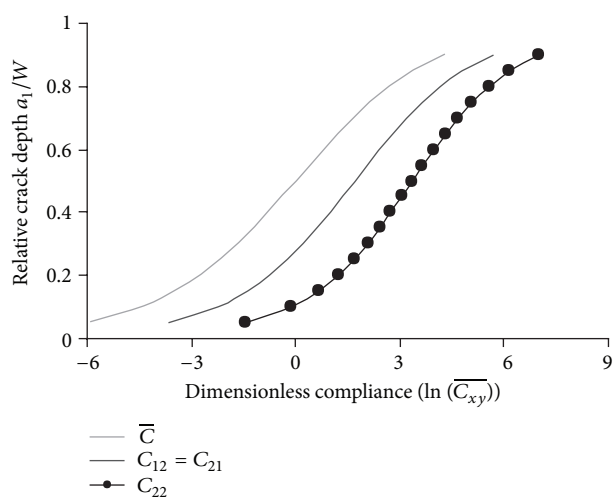

Figure 2: Relative crack depth (a_1/W) versus dimensionless compliance ($\ln(\overline{C_{xy}})$).

compression load for instability based on the variation of the first two resonant frequencies of the beam. Chondros et al. [8] have developed a continuous cracked beam vibration theory for the lateral vibration of cracked Euler-Bernoulli beams with single-edge or double-edge open cracks using the Hu-Washizu-Barr variational formulation.

A new method for natural frequency analysis of beam with an arbitrary number of cracks has been developed by Khiem and Lien [9] on the basis of the transfer matrix method and rotational spring model of crack. Cam et al. [10] have performed a study to obtain information about the location and depth of the cracks in cracked beam. Experimental and simulations results obtained are in good agreement. Zheng and Kessissoglou [11] have presented a method based on finite element method for detection of crack in faulty structural member. The results obtained from the proposed method are validated using experimental analysis. Tada et al. [12] have provided the basis for computation of compliance matrix for damage detection following fracture mechanics theory. Sekhar and Prabhu [13] have derived a method for crack detection in a cracked shaft using finite element analysis using correct expression for strain energy release rate function. Hossain et al. [14] have presented an investigation for comparative performance of intelligent system-like genetic algorithms (GAs) and adaptive neurofuzzy inference system (ANFIS) algorithms for identification of fault in an active vibration control (AVC) system. A comparative performance of the proposed method is presented and discussed through a set of experiments. Ranjbaran et al. [15] in their paper have formulated a method for vibration analysis of a beam

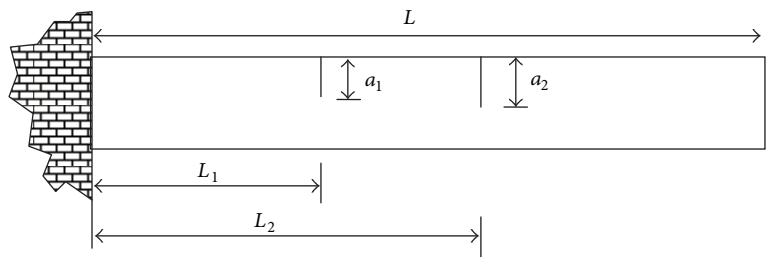

Figure 3

assuming the beam to be nonuniform. The vibration characteristics of the beam are computed and the results are compared with other methods. Zhou and Biegalski [16] have proposed a method to analyze the vibration signatures of a deck truss bridge with cracks at the gusset plate connecting the lower lateral bracing. In-service monitoring has been performed to measure the vibration properties of the truss and the lateral bracing members to avoid resonance with the excitation frequency. Wada et al. [18] have proposed a fuzzy control method with triangular type membership functions using an image processing unit to control the level of granules inside a hopper. They have stated that the image processing technique can be used as a detecting element, and with the use of fuzzy reasoning methods, good process responses are obtained. Pawar et al. [17] have used a genetic fuzzy system to identify the crack depth location in a composite matrix cracking model. As described by them, the genetic fuzzy system combines the uncertainty characteristics of fuzzy logic with the learning ability of genetic algorithm. Parhi [19] has designed a mobile robot navigation control system using fuzzy logic. Fuzzy rules embedded in the controller of a mobile robot enable it to avoid obstacles in a cluttered environment that includes other mobile robots.

In the present study, a finite element model for a cracked beam element is developed, and the results from theoretical and finite element analyses have been used to set the fuzzy rules. The fuzzy rules are used for designing the fuzzy inference system based on Gaussian membership function which is subsequently applied for prediction of damage in a faulty structure. The theoretical, finite element and fuzzy analysis are done to study the response of a cantilever beam in the presence of cracks. Theoretical results are compared with the experimental, fuzzy, and FEM results. A close agreement between the results has been observed.

2. Theoretical Analysis

2.1. Local Flexibility of a Cracked Beam under Bending and Axial Loading. The presence of a transverse surface crack of depth "a_1" and "a_2" on beam of width "B" and height "W" introduces a local flexibility, which can be defined in matrix form, the dimension of which depends on the degrees of freedom. Here, a 2×2 matrix is considered. A cantilever beam is subjected to axial force (P_1) and bending moment (P_2), shown in Figure 1(a), which gives coupling with the longitudinal and transverse motion. The cross-sectional view and the front view of the beam are shown in Figures 1(b) and 3, respectively.

The strain energy release rate at the fractured section can be written as follows [12]:

$$J = \frac{1}{E'}\left(K_{I1} + K_{I2}\right)^2, \tag{1}$$

where

$$\begin{aligned} \frac{1}{E'} &= \frac{1-\upsilon^2}{E'} \quad \text{(for plane strain condition)}, \\ \frac{1}{E'} &= \frac{1}{E} \quad \text{(for plane stress condition)} \end{aligned} \tag{2}$$

K_{I1} and K_{I2} are the stress intensity factors of mode I (opening of the crack) for loads P_1 and P_2, respectively. The values of stress intensity factors from earlier studies [12] are

$$K_{I1} = \frac{P_1}{BW}\sqrt{\pi a}\left(F_1\left(\frac{a}{W}\right)\right), \quad K_{I2} = \frac{6P_2}{BW^2}\sqrt{\pi a}\left(F_2\left(\frac{a}{W}\right)\right), \tag{3}$$

where expressions for F_1 and F_2 are as follows:

$$\begin{aligned} F_1\left(\frac{a}{W}\right) = {} & \left(\frac{2W}{\pi a}\tan\left(\frac{\pi a}{2W}\right)\right)^{0.5} \\ & \times\left\{\left(0.752+2.02\left(\frac{a}{W}\right)+0.37\left(1-\sin\left(\frac{\pi a}{2W}\right)\right)^3\right)\right. \\ & \left.\times\left(\cos\left(\frac{\pi a}{2W}\right)\right)^{-1}\right\}, \end{aligned} \tag{4}$$

$$\begin{aligned} F_2\left(\frac{a}{W}\right) = {} & \left(\frac{2W}{\pi a}\tan\left(\frac{\pi a}{2W}\right)\right)^{0.5} \\ & \times\left\{\left(0.923+0.199\left(1-\sin\left(\frac{\pi a}{2W}\right)\right)^4\right)\right. \\ & \left.\times\left(\cos\left(\frac{\pi a}{2W}\right)\right)^{-1}\right\}. \end{aligned} \tag{5}$$

Let U_t be the strain energy due to the crack. Then, from Castigliano's theorem, the additional displacement along the force P_i is

$$u_i = \frac{\partial U_t}{\partial P_i}. \tag{6}$$

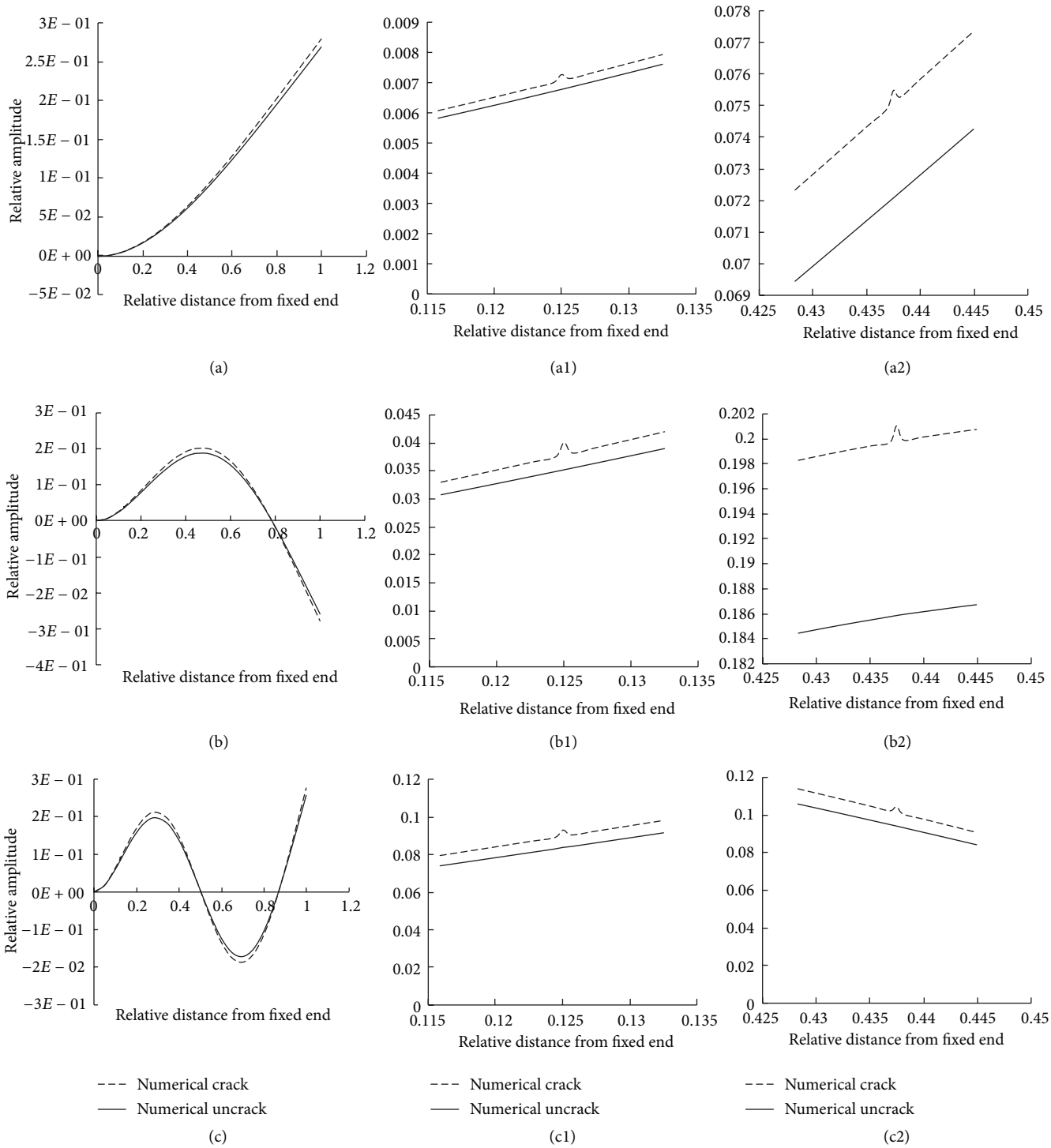

Figure 4: (a) Relative amplitude versus relative distance from the fixed end (1st mode of vibration), $a_1/W = 0.0833$, $a_2/W = 0.166$, $L_1/L = 0.125$, $L_2/L = 0.4375$. (a1) Magnified view of (a) at the vicinity of the crack location $L_1/L = 0.125$. (a2) Magnified view of (a) at the vicinity of the crack location $L_2/L = 0.4375$. (b) Relative amplitude versus relative distance from the fixed end (2nd mode of vibration), $a_1/W = 0.0833$, $a_2/W = 0.166$, $L_1/L = 0.125$, $L_2/L = 0.4375$. (b1) Magnified view of (b) at the vicinity of the crack location $L_1/L = 0.125$. (b2) Magnified view of (b) at the vicinity of the crack location $L_2/L = 0.4375$. (c) Relative amplitude versus relative distance from the fixed end (3rd mode of vibration), $a_1/W = 0.0833$, $a_2/W = 0.166$, $L_1/L = 0.125$, $L_2/L = 0.4375$. (c1) Magnified view of (c) at the vicinity of the crack location $L_1/L = 0.125$. (c2) Magnified view of (c) at the vicinity of the crack location $L_2/L = 0.4375$.

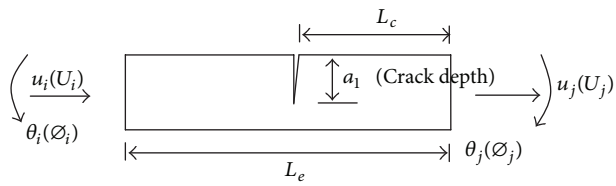

Figure 5: View of a crack beam element subjected to axial and bending forces.

The strain energy will have the form

$$U_t = \int_0^{a_1} \frac{\partial U_t}{\partial a} da = \int_0^{a_1} J da, \tag{7}$$

where $J = \partial U_t / \partial a$ is the strain energy density function.

From (1) and (4), thus we have

$$u_i = \frac{\partial}{\partial P_i} \left[\int_0^{a_1} J(a)\, da \right]. \tag{8}$$

The flexibility influence coefficient C_{ij} will be, by definition,

$$C_{ij} = \frac{\partial u_i}{\partial P_j} = \frac{\partial^2}{\partial P_i \partial P_j} \int_0^{a_1} J(a)\, da \tag{9}$$

and can be written as

$$C_{ij} = \frac{BW}{E'} \frac{\partial^2}{\partial P_i \partial P_j} \int_0^{\xi_1} \left(K_{I1} + K_{I2}\right)^2 d\xi. \tag{10}$$

From (9), calculating C_{11}, C_{12} (=C_{21}), and C_{22}, we get

$$\overline{C_{11}} = C_{11} \frac{BE'}{2\pi}; \quad \overline{C_{12}} = C_{12} \frac{E'BW}{12\pi} = \overline{C_{21}}; \quad \overline{C_{22}} = C_{22} \frac{E'BW^2}{72\pi}. \tag{11}$$

The local stiffness matrix can be obtained by taking the inversion of compliance matrix. That is,

$$K = \begin{bmatrix} K_{11} & K_{12} \\ K_{21} & K_{22} \end{bmatrix} = \begin{bmatrix} C_{11} & C_{12} \\ C_{21} & C_{22} \end{bmatrix}^{-1}. \tag{12}$$

Figure 2 shows the variation of dimensionless compliances to that of relative crack depth.

2.2. Analysis of Vibration Characteristics of the Cracked Beam. A cantilever beam of length "L", width "B", and depth "W", with a crack of depth "a_1" and "a_2" at a distance "L_1" and "L_2", respectively, from the fixed end, is considered (shown in Figure 1). Taking $u_1(x,t)$, $u_2(x,t)$, and $u_3(x,t)$ as the amplitudes of longitudinal vibration for the sections before, in-between, and after the crack, $y_1(x,t)$, $y_2(x,t)$, and $y_3(x,t)$ are the amplitudes of bending vibration for the same sections.

The normal function for the system can be defined as

$$\begin{aligned}
\overline{u}_1(\overline{x}) &= A_1 \cos\left(\overline{K}_u \overline{x}\right) + A_2 \sin\left(\overline{K}_u \overline{x}\right), \\
\overline{u}_2(\overline{x}) &= A_3 \cos\left(\overline{K}_u \overline{x}\right) + A_4 \sin\left(\overline{K}_u \overline{x}\right), \\
\overline{u}_3(\overline{x}) &= A_5 \cos\left(\overline{K}_u \overline{x}\right) + A_6 \sin\left(\overline{K}_u \overline{x}\right), \\
\overline{y}_1(\overline{x}) &= A_7 \cosh\left(\overline{K}_y \overline{x}\right) + A_8 \sinh\left(\overline{K}_y \overline{x}\right) + A_9 \cos\left(\overline{K}_y \overline{x}\right) \\
&\quad + A_{10} \sin\left(\overline{K}_y \overline{x}\right), \\
\overline{y}_2(\overline{x}) &= A_{11} \cosh\left(\overline{K}_y \overline{x}\right) + A_{12} \sinh\left(\overline{K}_y \overline{x}\right) + A_{13} \cos\left(\overline{K}_y \overline{x}\right) \\
&\quad + A_{14} \sin\left(\overline{K}_y \overline{x}\right), \\
\overline{y}_3(\overline{x}) &= A_{15} \cosh\left(\overline{K}_y \overline{x}\right) + A_{16} \sinh\left(\overline{K}_y \overline{x}\right) + A_{17} \cos\left(\overline{K}_y \overline{x}\right) \\
&\quad + A_{18} \sin\left(\overline{K}_y \overline{x}\right),
\end{aligned} \tag{13}$$

where $\overline{x} = x/L$, $\overline{u} = u/L$, $\overline{y} = y/L$, $\beta_1 = L_1/L$, $\beta_2 = L_2/L$, $\overline{K}_u = \omega L / C_u$, $C_u = (E/\rho)^{1/2}$, $\overline{K}_y = (\omega L^2 / C_y)^{1/2}$, $C_y = (EI/\mu)^{1/2}$, and $\mu = A\rho$, A_i, $(i = 1, \ldots, 18)$. Constants are to be determined from boundary conditions. The boundary conditions of the cantilever beam in consideration are

$$\begin{aligned}
&\overline{u}_1(0) = 0; \quad \overline{y}_1(0) = 0; \quad \overline{y}_1'(0) = 0; \\
&\overline{u}_3'(1) = 0; \quad \overline{y}_3''(1) = 0; \quad \overline{y}_3'''(1) = 0.
\end{aligned} \tag{14}$$

At the cracked section

$$\begin{aligned}
&\overline{u}_1'(\beta_1) = \overline{u}_2'(\beta_1); \quad \overline{y}_1(\beta_1) = \overline{y}_2(\beta_1); \\
&\overline{y}_1''(\beta_1) = \overline{y}_2''(\beta_1); \quad \overline{y}_1'''(\beta_1) = \overline{y}_2'''(\beta_1), \\
&\overline{u}_2'(\beta_2) = \overline{u}_3'(\beta_2); \quad \overline{y}_2(\beta_2) = \overline{y}_3(\beta_2); \\
&\overline{y}_2''(\beta_2) = \overline{y}_3''(\beta_2); \quad \overline{y}_2'''(\beta_2) = \overline{y}_3'''(\beta_2).
\end{aligned} \tag{15}$$

Also, at the cracked section L_1, we have

$$\begin{aligned}
AE \frac{du_1(L_1)}{dx} &= K_{11}\left(u_2(L_1) - u_1(L_1)\right) \\
&\quad + K_{12}\left(\frac{dy_2(L_1)}{dx} - \frac{dy_1(L_1)}{dx}\right).
\end{aligned} \tag{16}$$

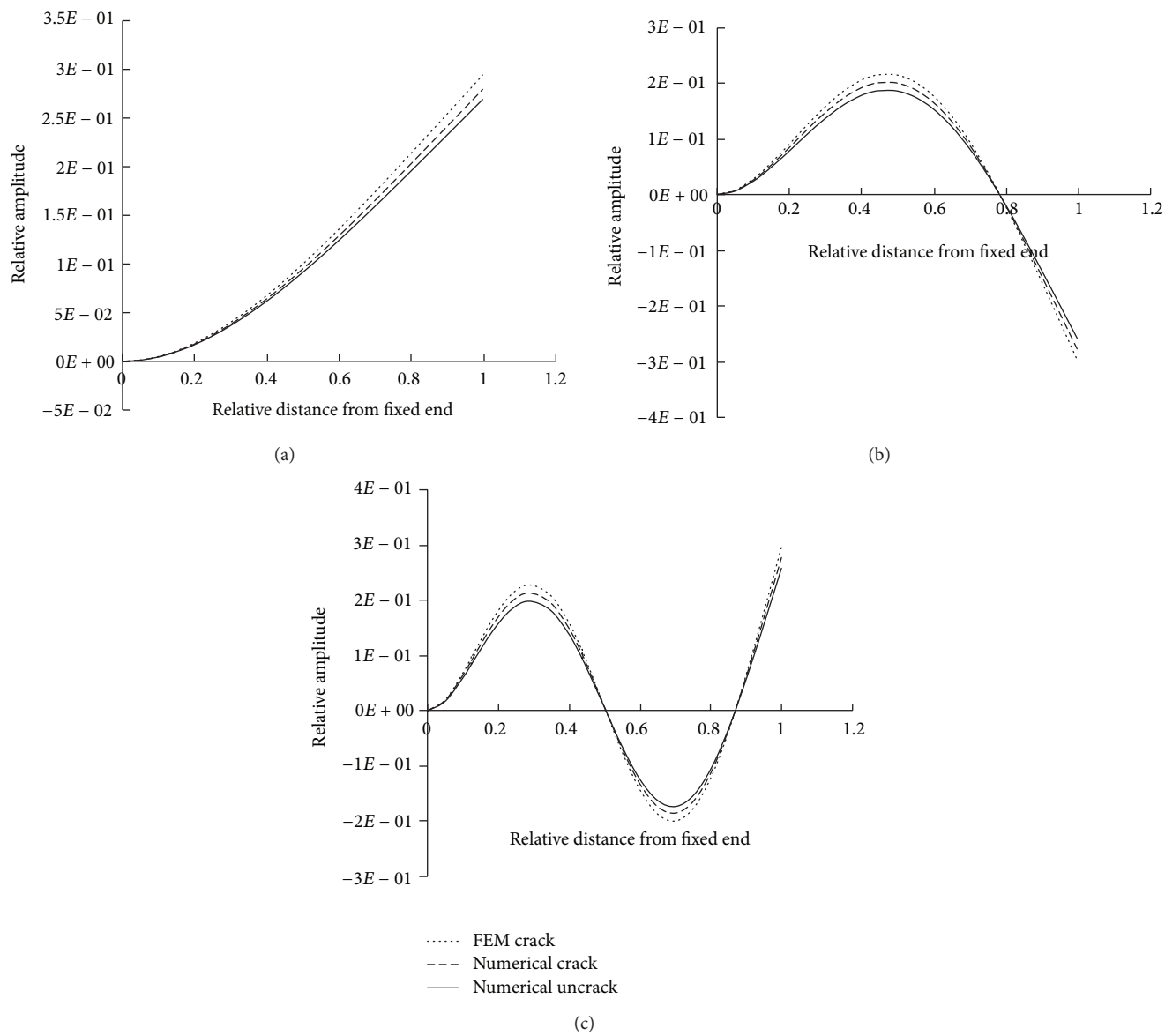

Figure 6: (a) Relative amplitude versus relative distance from the fixed end (1st mode of vibration), $a_1/W = 0.0833$, $a_2/W = 0.166$, $L_1/L = 0.125$, $L_2/L = 0.4375$. (b) Relative amplitude versus relative distance from the fixed end (2nd mode of vibration), $a_1/W = 0.0833$, $a_2/W = 0.166$, $L_1/L = 0.125$, $L_2/L = 0.4375$. (c) Relative amplitude versus relative distance from the fixed end (3rd mode of vibration), $a_1/W = 0.0833$, $a_2/W = 0.166$, $L_1/L = 0.125$, $L_2/L = 0.4375$.

Multiplying both sides of the previous equation by $AE/LK_{11}K_{12}$, we get

$$M_1 M_2 \overline{u}_1'(\beta_1) = M_2(\overline{u}_2(\beta_1) - \overline{u}_1(\beta_1)) + M_1\left(\overline{y}_2'(\beta_1) - \overline{y}_1'(\beta_1)\right). \tag{17}$$

Similarly,

$$EI\frac{d^2 y_1(L_1)}{dx^2} = K_{21}(u_2(L_1) - u_1(L_1)) + K_{22}\left(\frac{dy_2(L_1)}{dx} - \frac{dy_1(L_1)}{dx}\right). \tag{18}$$

Multiplying both sides of the previous equation by $EI/L^2K_{22}K_{21}$, we get

$$M_3 M_4 \overline{y}_1''(\beta_1) = M_3(\overline{u}_2(\beta_1) - \overline{u}_1(\beta_1)) + M_4\left(\overline{y}_2'(\beta_1) - \overline{y}_1'(\beta_1)\right), \tag{19}$$

where

$$M_1 = \frac{AE}{LK_{11}}, \quad M_2 = \frac{AE}{K_{12}}, \quad M_3 = \frac{EI}{LK_{22}}, \quad M_4 = \frac{EI}{L^2K_{21}}. \tag{20}$$

Table 1: Description of fuzzy linguistic terms.

Membership functions name	Linguistic terms	Description and range of the linguistic terms
L1F1, L1F2, L1F3, L1F4	$fnf_{1\ to\ 4}$	Low ranges of relative natural frequency for first mode of vibration in descending order, respectively.
M1F1, M1F2	$fnf_{5,6}$	Medium ranges of relative natural frequency for first mode of vibration in ascending order, respectively.
H1F1, H1F2, H1F3, H1F4	$fnf_{7\ to\ 10}$	Higher ranges of relative natural frequency for first mode of vibration in ascending order, respectively.
L2F1, L2F2, L2F3, L2F4	$snf_{1\ to\ 4}$	Low ranges of relative natural frequency for second mode of vibration in descending order, respectively.
M2F1, M2F2	$snf_{5,6}$	Medium ranges of relative natural frequency for second mode of vibration in ascending order, respectively.
H2F1, H2F2, H2F3, H2F4	$snf_{7\ to\ 10}$	Higher ranges of relative natural frequencies for second mode of vibration in ascending order, respectively.
L3F1, L3F2, L3F3, L3F4	$tnf_{1\ to\ 4}$	Low ranges of relative natural frequencies for third mode of vibration in descending order, respectively.
M3F1, M3F2	$tnf_{5,6}$	Medium ranges of relative natural frequencies for third mode of vibration in ascending order, respectively.
H3F1, H3F2, H3F3, H3F4	$tnf_{7\ to\ 10}$	Higher ranges of relative natural frequencies for third mode of vibration in ascending order, respectively.
S1M1, S1M2, S1M3, S1M4	$fmd_{1\ to\ 4}$	Small ranges of first relative mode shape difference in descending order, respectively.
M1M1, M1M2	$fmd_{5,6}$	Medium ranges of first relative mode shape difference in ascending order, respectively.
H1M1, H1M2, H1M3, H1M4	$fmd_{7\ to\ 10}$	Higher ranges of first relative mode shape difference in ascending order, respectively.
S2M1, S2M2, S2M3, S2M4	$smd_{1\ to\ 4}$	Small ranges of second relative mode shape difference in descending order, respectively.
M2M1, M2M2	$smd_{5,6}$	Medium ranges of second relative mode shape difference in ascending order, respectively.
H2M1, H2M2, H2M3, H2M4	$smd_{7\ to\ 10}$	Higher ranges of second relative mode shape difference in ascending order, respectively.
S3M1, S3M2, S3M3, S3M4	$tmd_{1\ to\ 4}$	Small ranges of third relative mode shape difference in descending order, respectively.
M3M1, M3M2	$tmd_{5,6}$	Medium ranges of third relative mode shape difference in ascending order, respectively.
H3M1, H3M2, H3M3, H3M4	$tmd_{7\ to\ 10}$	Higher ranges of third relative mode shape difference in ascending order, respectively.
S1L1, S1L2,. . ., S1L22	$rcl1_{1\ to\ 22}$	Small ranges of relative crack location in descending order, respectively.
M1L1, M1L2	$rcl1_{23,24}$	Medium ranges of relative crack location in ascending order, respectively.
B1L1, B1L2,. . ., B1L22	$rcl1_{25\ to\ 46}$	Bigger ranges of relative crack location in ascending order, respectively.
S1D1, S1D2,. . ., S1D9	$rcd1_{1\ to\ 9}$	Small ranges of relative crack depth in descending order, respectively.
M1D	$rcd1_{10}$	Medium relative crack depth.
L1D1, L1D2,. . ., L1D9	$rcd1_{11\ to\ 19}$	Larger ranges of relative crack depth in ascending order, respectively.
S2L1, S2L2,. . ., S2L22	$rcl2_{1\ to\ 22}$	Small ranges of relative crack location in descending order, respectively.
M2L1, M2L2	$rcl2_{23,24}$	Medium ranges of relative crack location in ascending order, respectively.
B2L1, B2L2,. . ., B2L22	$rcl2_{25\ to\ 46}$	Bigger ranges of relative crack location in ascending order, respectively.
S2D1, S2D2,. . ., S2D9	$rcd2_{1\ to\ 9}$	Small ranges of relative crack depth in descending order, respectively.
M2D	$rcd2_{10}$	Medium relative crack depth.
L2D1, L2D2,. . ., L2D9	$rcd2_{11\ to\ 19}$	Larger ranges of relative crack depth in ascending order, respectively.

Table 2: Examples of twenty fuzzy rules used in fuzzy controller.

Sl. No.	Examples of some rules used in the fuzzy controller
1	If fnf is H1F1, snf is M2F2, tnf is M3F1, fmd is H1M2, smd is H2M4, tmd is H3M3, then rcd1 is S1D6, and rcl1 is S1L17, and rcd2 is S2D4, and rcl2 is S2L6.
2	If fnf is L1F4, snf is L2F4, tnf is L3F4, fmd is H1M1, smd is H2M1, tmd is H3M2, then rcd1 is S1D2, and rcl1 is S1L17, and rcd2 is S2D1, and rcl2 is M2L2.
3	If fnf is L1F3, snf is L2F4, tnf is L3F4, fmd is M1M2, smd is H2M2, tmd is H3M3, then rcd1 is M1D, and rcl1 is S1L17, and rcd2 is S2D2, and rcl2 is B2L19.
4	If fnf is H1F2, snf is H2F1, tnf is H3F1, fmd is H1M3, smd is H2M4, tmd is H3M4, then rcd1 is S1D6, and rcl1 is S1L11, and rcd2 is S2D4, and rcl2 is M2L2.
5	If fnf is M1F1, snf is L2F2, tnf is L3F3, fmd is H1M1, smd is H2M1, tmd is H3M2, then rcd1 is S1D4, and rcl1 is S1L11, and rcd2 is S2D1, and rcl2 is B2L13.
6	If fnf is L1F1, snf is L2F2, tnf is L3F3, fmd is H1M3, smd is M2M1, tmd is H3M4, then rcd1 is M1D, and rcl1 is S1L11, and rcd2 is S2D7, and rcl2 is M2L2.
7	If fnf is L1F4, snf is L2F4, tnf is L3F4, fmd is M1M2, smd is H2M1, tmd is H3M1, then rcd1 is L1D1, and rcl1 is S1L11, and rcd2 is S2D4, and rcl2 is B2L10.
8	If fnf is H1F1, snf is M2F2, tnf is M3F1, fmd is H1M2, smd is H2M2, tmd is H3M2, then rcd1 is S1D6, and rcl1 is S1L6, and rcd2 is S2D4, and rcl2 is B2L5.
9	If fnf is L1F1, snf is L2F4, tnf is L3F4, fmd is M1M1, smd is M2M1, tmd is M3M2, then rcd1 is S1D2, and rcl1 is S1L6, and rcd2 is L2D1, and rcl2 is B2L5.
10	If fnf is M1F1, snf is L2F2, tnf is L3F1, fmd is M1M2, smd is M2M2, tmd is H3M1, then rcd1 is S1D1, and rcl1 is S1L6, and rcd2 is S2D4, and rcl2 is B2L5.
11	If fnf is M1F1, snf is M2F1, tnf is M3F1, fmd is H1M3, smd is H2M3, tmd is H3M4, then rcd1 is S1D6, and rcl1 is S1L18, and rcd2 is S2D5, and rcl2 is M2L2.
12	If fnf is M1F1, snf is L2F1, tnf is L3F1, fmd is H1M3, smd is H2M2, tmd is H3M3, then rcd1 is S1D4, and rcl1 is S1L17, and rcd2 is S2D6, and rcl2 is S2L6.
13	If fnf is M1F2, snf is M2F1, tnf is M3F1, fmd is M1M1, smd is H2M1, tmd is H3M2, then rcd1 is S1D4, and rcl1 is S1L11, and rcd2 is S2D4, and rcl2 is M2L2.
14	If fnf is H1F2, snf is H2F1, tnf is H3F1, fmd is H1M4, smd is H2M1, tmd is H3M1, then rcd1 is S1D7, and rcl1 is S1L17, and rcd2 is S2D6, and rcl2 is B2L16.
15	If fnf is M1F1, snf is L2F1, tnf is L3F2, fmd is S1M1, smd is S2M2, tmd is H3M1, then rcd1 is S1D2, and rcl1 is S1L11, and rcd2 is S2D6, and rcl2 is B2L10.
16	If fnf is L1F4, snf is L2F4, tnf is L3F4, fmd is H1M2, smd is S2M1, tmd is H3M2, then rcd1 is L1D1, and rcl1 is S1L17, and rcd2 is S2D5, and rcl2 is M2L2.
17	If fnf is M1F1, snf is L2F3, tnf is L3F1, fmd is S1M2, smd is M2M1, tmd is S3M1, then rcd1 is S1D6, and rcl1 is S1L12, and rcd2 is M2D, and rcl2 is M2L1.
18	If fnf is L1F1, snf is L2F1, tnf is L3F1, fmd is H1M2, smd is H2M2, tmd is H3M2, then rcd1 is S1D2, and rcl1 is S1L12, and rcd2 is S2D4, and rcl2 is B2L13.
19	If fnf is H1F2, snf is H2F1, tnf is H3F1, fmd is S1M2, smd is H2M3, tmd is H3M1, then rcd1 is S1D4, and rcl1 is S1L5, and rcd2 is S2D6, and rcl2 is B2L6.
20	If fnf is L1F3, snf is L2F4, tnf is L3F4, fmd is S1M3, smd is S2M2, tmd is S3M3, then rcd1 is L1D1, and rcl1 is S1L5, and rcd2 is S2D2, and rcl2 is B2L5.

Similarly, at the crack section L_2, we can have the expression

$$\begin{aligned} M_1 M_2 \overline{u}_2'(\beta_2) &= M_2(\overline{u}_3(\beta_2) - \overline{u}_2(\beta_2)) \\ &\quad + M_1\left(\overline{y}_3'(\beta_2) - \overline{y}_2'(\beta_2)\right), \\ M_3 M_4 \overline{y}_2''(\beta_2) &= M_3(\overline{u}_3(\beta_2) - \overline{u}_2(\beta_2)) \\ &\quad + M_4\left(\overline{y}_3'(\beta_2) - \overline{y}_2'(\beta_2)\right). \end{aligned} \tag{21}$$

The normal functions in (13) along with the boundary conditions as mentioned earlier yield the characteristic equation of the system as

$$|Q| = 0. \tag{22}$$

This determinant is a function of natural circular frequency (ω), the relative locations of the crack (β_1, β_2), and the local stiffness matrix (K) which in turn is a function of the relative crack depth ($a_1/W, a_2/W$).

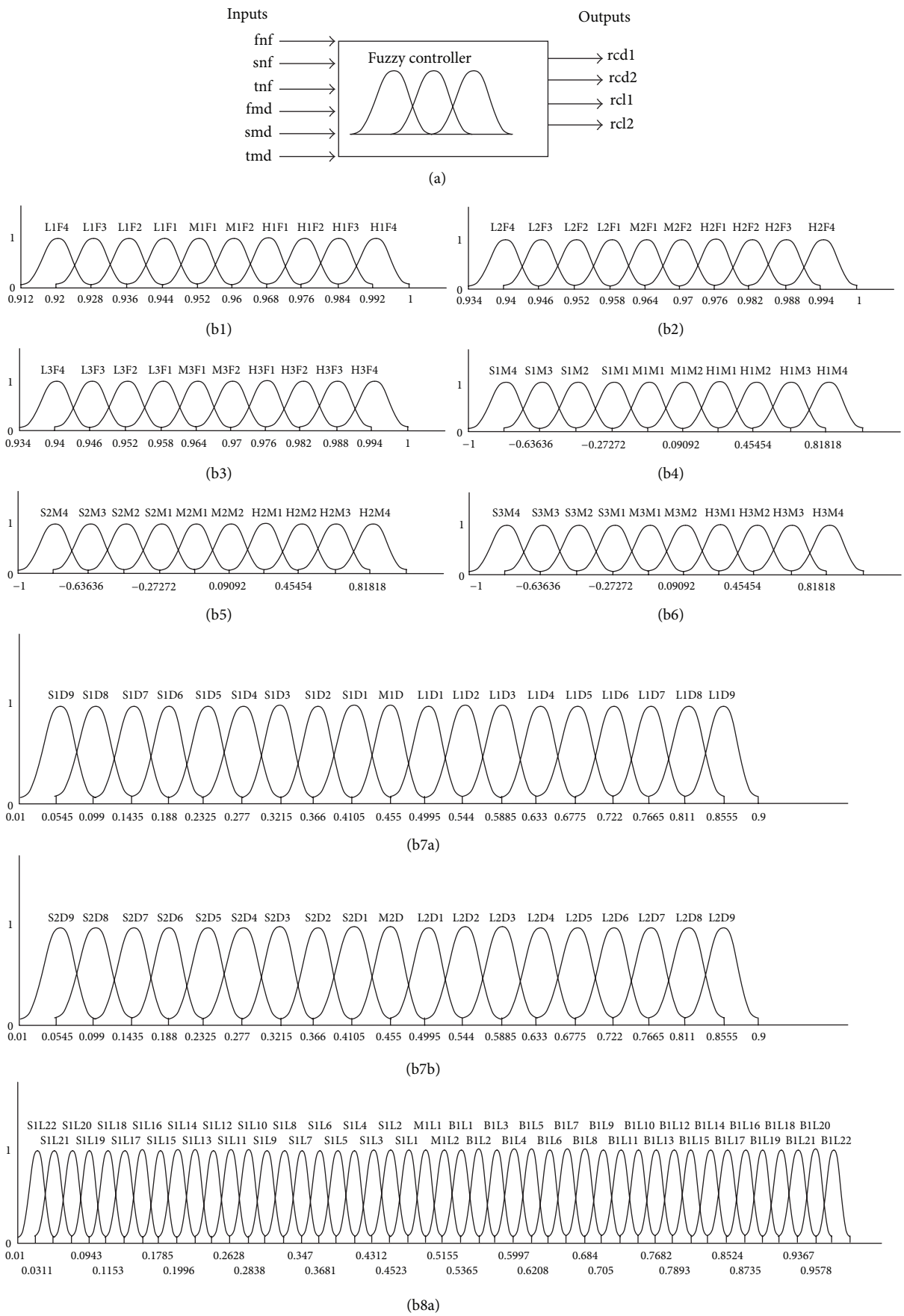

Figure 7: Continued.

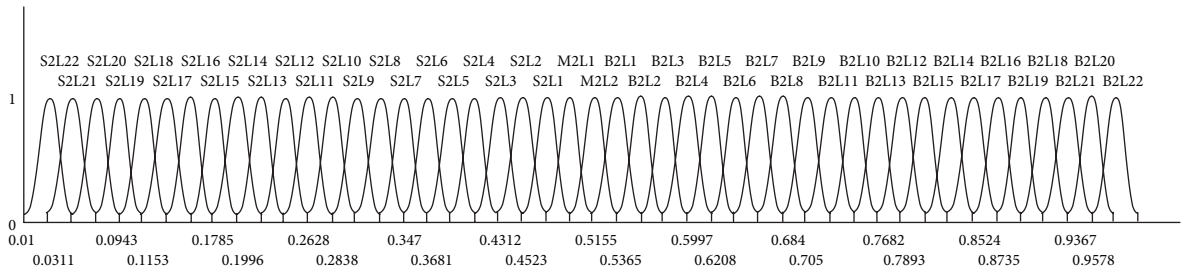

(b8b)

Figure 7: (a) Fuzzy controller. (b1) Membership functions for relative natural frequency for first mode of vibration. (b2) Membership functions for relative natural frequency for second mode of vibration. (b3) Membership functions for relative natural frequency for third mode of vibration. (b4) Membership functions for relative mode shape difference for first mode of vibration. (b5) Membership functions for relative mode shape difference for second mode of vibration. (b6) Membership functions for relative mode shape difference for third mode of vibration. (b7a) Membership functions for relative crack depth 1. (b7b) Membership functions for relative crack depth 2. (b8a) Membership functions for relative crack location 1. (b8b) Membership functions for relative crack location 2.

The results of the theoretical analysis for the first three mode shapes for uncracked and cracked beams are shown in Figure 4.

3. Analysis of Cracked Beam Using Finite Element Method (FEM)

In the following section, FEM is analyzed for vibration analysis of a cantilever cracked beam (Figure 5). The relationship between the displacement and the forces can be expressed as

$$\begin{Bmatrix} u_j - u_i \\ \theta_j - \theta_i \end{Bmatrix} = C_{\text{ovl}} \begin{Bmatrix} U_j \\ \emptyset_j \end{Bmatrix}, \tag{23}$$

where overall flexibility matrix C_{ovl} can be expressed as

$$C_{\text{ovl}} = \begin{bmatrix} C_{11} & -C_{12} \\ -C_{21} & C_{22} \end{bmatrix}. \tag{24}$$

The displacement vector in (23) is due to the crack.

The forces acting on the beam element for FEM analysis are shown in Figure 5.

Under this system, the flexibility matrix C_{intact} of the intact beam element can be expressed as

$$\begin{Bmatrix} u_j - u_i \\ \theta_j - \theta_i \end{Bmatrix} = C_{\text{intact}} \begin{Bmatrix} U_j \\ \emptyset_j \end{Bmatrix}, \tag{25}$$

where $C_{\text{intact}} = \begin{bmatrix} Le/EA & 0 \\ 0 & Le/EI \end{bmatrix}$.

The displacement vector in (25) is for the intact beam.

The total flexibility matrix C_{tot} of the cracked beam element can now be obtained by

$$C_{\text{tot}} = C_{\text{intact}} + C_{\text{ovl}} = \begin{bmatrix} \dfrac{Le}{EA} + C_{11} & -C_{12} \\ -C_{21} & \dfrac{Le}{EI} + C_{22} \end{bmatrix}. \tag{26}$$

Through the equilibrium conditions, the stiffness matrix K_c of a cracked beam element can be obtained as follows [13]:

$$K_c = DC_{\text{tot}}^{-1}D^T, \tag{27}$$

where D is the transformation matrix and is expressed as

$$D = \begin{bmatrix} -1 & 0 \\ 0 & -1 \\ 1 & 0 \\ 0 & 1 \end{bmatrix}. \tag{28}$$

The results of the finite element analysis for the first three mode shapes of the cracked beam are compared with that of the numerical analysis of the cracked beam and are presented in Figure 6.

4. Analysis of the Fuzzy Controller

The fuzzy controller developed has got six input parameters and two output parameters.

The linguistic terms used for the inputs are as follows:

relative first natural frequency = "fnf"; relative second natural frequency = "snf";

relative third natural frequency = "tnf";

average relative first mode shape difference = "fmd";

average relative second mode shape difference = "smd";

average relative third mode shape difference = "tmd".

The linguistic terms used for the outputs are as follows:

first relative crack location = "rcl1" and first relative crack depth = "rcd1";

second relative crack location = "rcl2" and second relative crack depth = "rcd2".

The fuzzy controller used in the present text is shown in Figure 7(a). The Gaussian membership functions are shown pictorially in Figure 7(b). The linguistic terms for the Gaussian membership functions, used in the fuzzy controller, are described in Table 1.

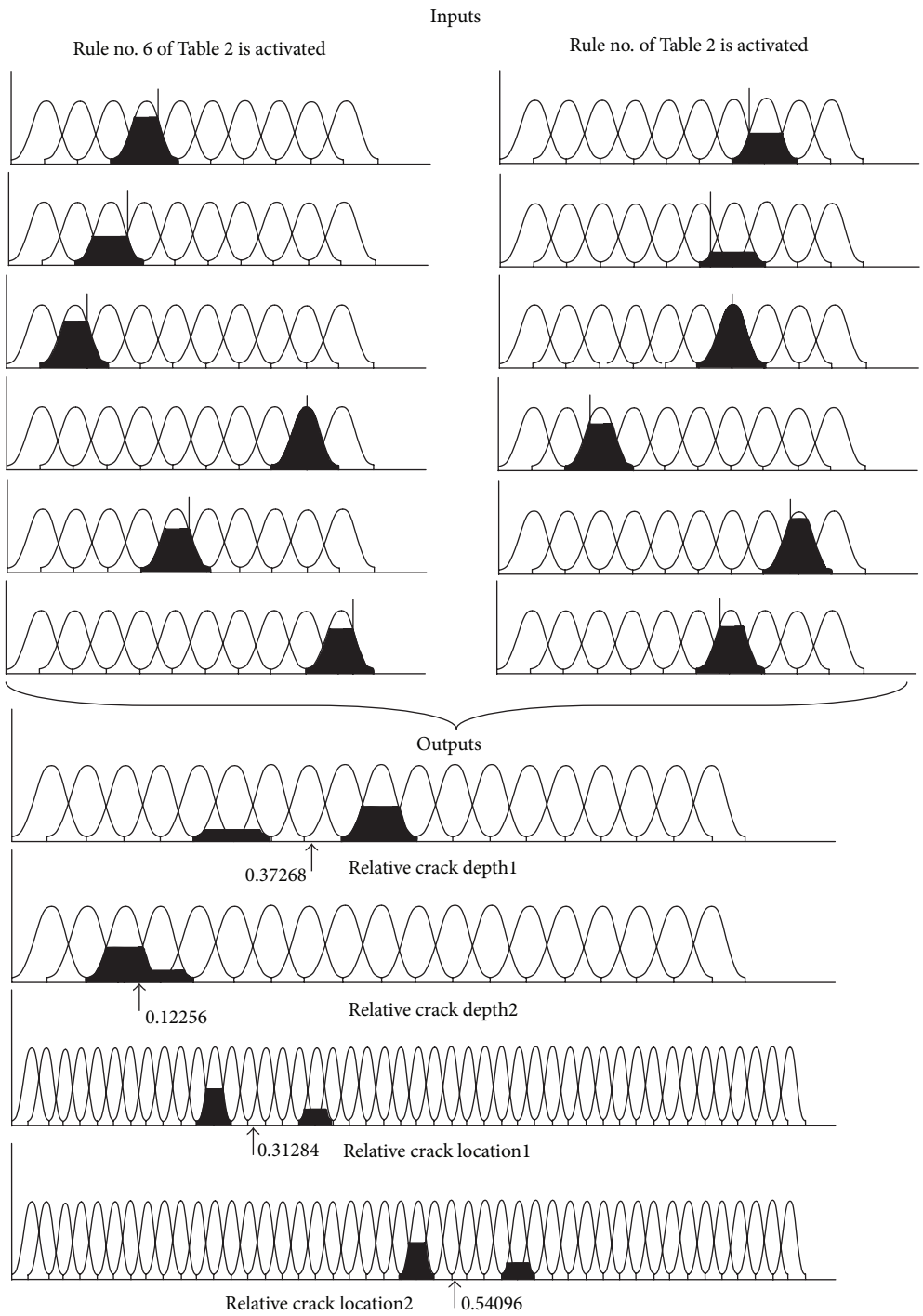

Figure 8: Resultant values of relative crack depth and relative crack location when rules 6 and 19 of Table 2 are activated.

4.1. Fuzzy Mechanism for Crack Detection. Based on the previous fuzzy subsets, the fuzzy control rules are defined in a general form as follows:

$$\begin{aligned} &\text{If fnf is fnf}_i \text{ and snf is snf}_j \text{ and tnf is tnf}_k \\ &\quad \text{and fmd is fmd}_l \text{ and smd is smd}_m \text{ and tmd is tmd}_n, \\ &\text{then rcl1 is rcl1}_{ijklmn} \text{ and rcd1 is rcd1}_{ijklmn} \\ &\quad \text{and rcl2 is rcl2}_{ijklmn} \text{ and rcd2 is rcd2}_{ijklmn}, \end{aligned} \tag{29}$$

where $i = 1$ to 10, $j = 1$ to 10, $k = 1$ to 10, $l = 1$ to 10, $m = 1$ to 10, and $n = 1$ to 10 because "fnf," "snf," "tnf," "fmd," "smd," and "tmd" have ten membership functions each.

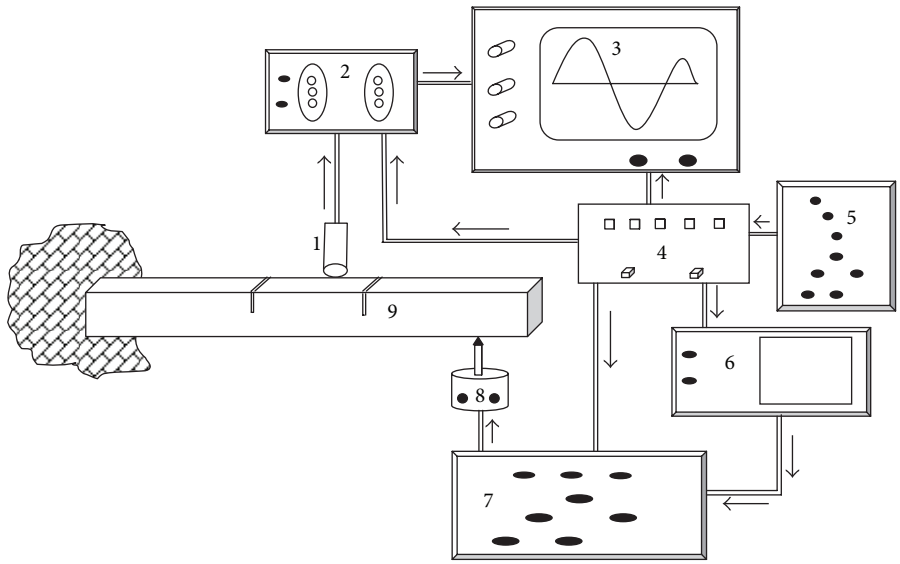

(1) Vibration pickup (accelerometer)
(2) Vibration analyzer (PULSE lite type 3560L)
(3) Vibration indicator with software (PULSE lab shop software)
(4) Distribution box
(5) Power supply
(6) Function generator
(7) Power amplifier
(8) Vibration exciter
(9) Cantilever beam specimen

Figure 9: Schematic block diagram of experimental setup.

From expression (29), two sets of rules can be written:

If fnf is fnf_i and snf is snf_j and tnf is tnf_k

and fmd is fmd_l and smd is smd_m and tmd is tmd_n,

then rcd1 is rcd1_{ijklmn} and rcd2 is rcd2_{ijklmn};

If fnf is fnf_i and snf is snf_j and tnf is tnf_k

and fmd is fmd_l and smd is smd_m and tmd is tmd_n,

then rcl1 is rcl1_{ijklmn} and rcl2 is rcl2_{ijklmn}. (30)

According to the usual fuzzy logic control method [19], a factor W_{ijklmn} is defined for the rules as follows:

$$\begin{aligned} W_{ijklmn} = {} & \mu_{\text{fnf}_i}(\text{freq}_i) \wedge \mu_{\text{snf}_j}(\text{freq}_j) \wedge \mu_{\text{tnf}_k}(\text{freq}_k) \\ & \wedge \mu_{\text{fmd}_l}(\text{moddif}_l) \wedge \mu_{\text{smd}_m}(\text{moddif}_m) \\ & \wedge \mu_{\text{tmd}_n}(\text{moddif}_n), \end{aligned} \tag{31}$$

where freq_i, freq_j, and freq_k are the first, second, and third relative natural frequencies of the cantilever beam with crack, respectively; moddif_l, moddif_m, and moddif_n are the average first, second, and third relative mode shape differences of the cantilever beam with crack, respectively. By applying the composition rule of inference [19], the membership values of the relative crack location and relative crack depth, $(\text{location})_{\text{rcl}\upsilon}$ and $(\text{depth})_{\text{rcd}\upsilon}$ $(\upsilon = 1, 2)$, can be computed as

$$\begin{aligned} & \mu_{\text{rcl}\upsilon_{ijklmn}}(\text{location}) \\ & \quad = W_{ijklmn} \wedge \mu_{\text{rcl}\upsilon_{ijklmn}}(\text{location}) \quad \forall \text{ length} \in \text{rcl}\upsilon, \\ & \mu_{\text{rcd}\upsilon_{ijklmn}}(\text{depth}) \\ & \quad = W_{ijklmn} \wedge \mu_{\text{rcd}\upsilon_{ijklmn}}(\text{depth}) \quad \forall \text{ depth} \in \text{rcd}\upsilon. \end{aligned} \tag{32}$$

The overall conclusion by combining the outputs of all the fuzzy rules can be written as follows:

$$\begin{aligned} \mu_{\text{rcl}\upsilon}(\text{location}) = {} & \mu_{\text{rcl}\upsilon_{111111}}(\text{location}) \\ & \vee \cdots \vee \mu_{\text{rcl}\upsilon_{ijklmn}}(\text{location}) \\ & \vee \cdots \vee \mu_{\text{rcl}\upsilon_{10101010101010}}(\text{location}), \\ \mu_{\text{rcd}\upsilon}(\text{depth}) = {} & \mu_{\text{rcd}\upsilon_{111111}}(\text{depth}) \vee \cdots \vee \mu_{\text{rcd}\upsilon_{ijklmn}}(\text{depth}) \\ & \vee \cdots \vee \mu_{\text{rcd}\upsilon_{10101010101010}}(\text{depth}). \end{aligned} \tag{33}$$

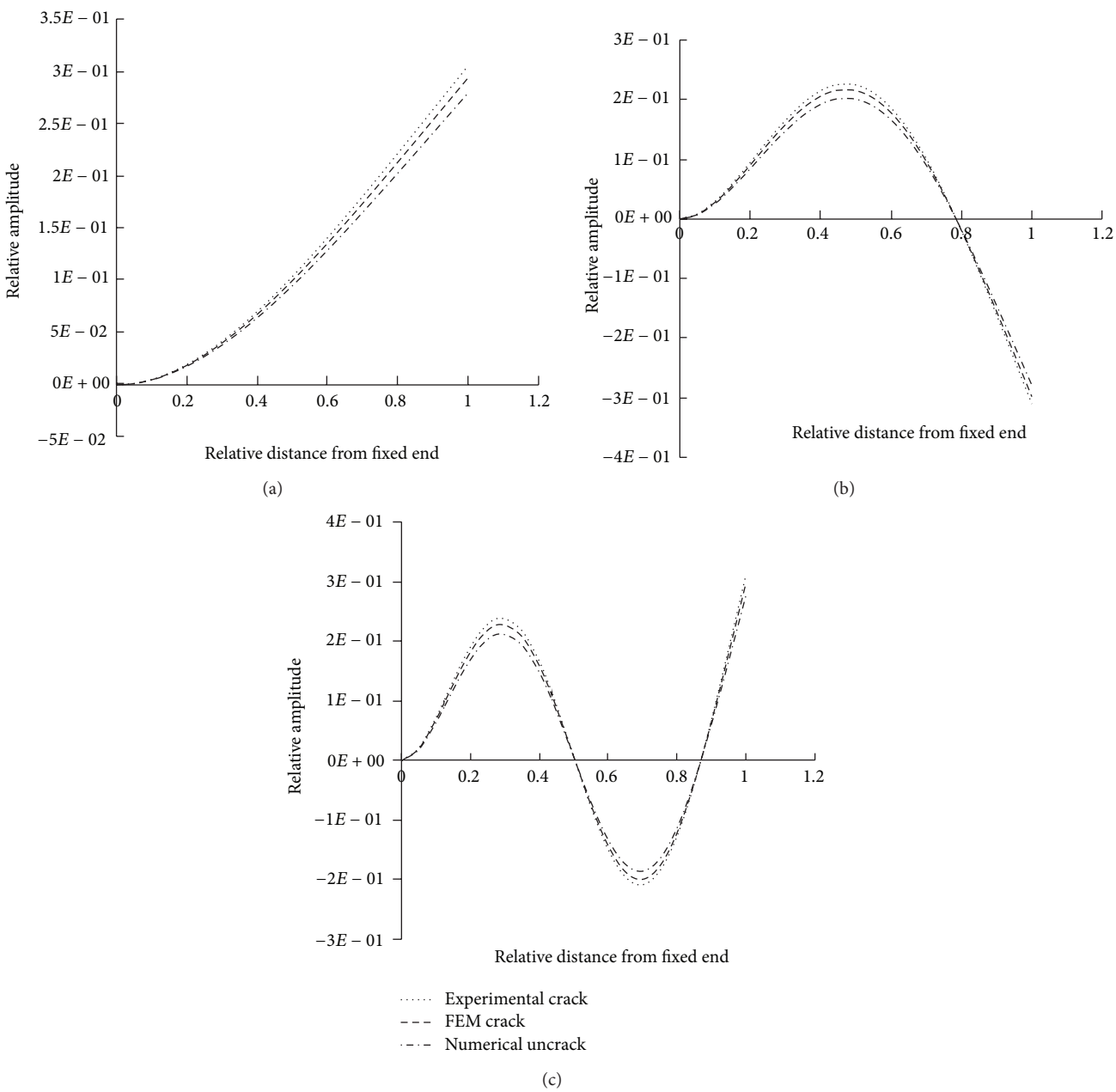

Figure 10: (a) Relative amplitude versus relative distance from the fixed end (1st mode of vibration), $a_1/W = 0.0833$, $a_2/W = 0.166$, $L_1/L = 0.125$, $L_2/L = 0.4375$. (b) Relative amplitude versus relative distance from the fixed end (2nd mode of vibration), $a_1/W = 0.0833$, $a_2/W = 0.166$, $L_1/L = 0.125$, $L_2/L = 0.4375$. (c) Relative amplitude versus relative distance from the fixed end (3rd mode of vibration), $a_1/W = 0.0833$, $a_2/W = 0.166$, $L_1/L = 0.125$, $L_2/L = 0.4375$.

The crisp values of relative crack location and relative crack depth are computed using the centre of gravity method [19] as

$$\text{relative crack location} = \text{rcl}\,1,2 = \frac{\int (\text{location}) \cdot \mu_{\text{rcl1,2}}(\text{location}) \cdot d\,(\text{location})}{\int \mu_{\text{rcl1,2}}(\text{location}) \cdot d\,(\text{location})},$$

$$\text{relative crack depth} = \text{rcd}\,1,2 = \frac{\int (\text{depth}) \cdot \mu_{\text{rcd1,2}}(\text{depth}) \cdot d\,(\text{depth})}{\int \mu_{\text{rcd1,2}}(\text{depth}) \cdot d\,(\text{depth})}. \tag{34}$$

4.2. Fuzzy Controller for Finding out Crack Depth and Crack Location. The inputs to the fuzzy controller are relative first natural frequency, relative second natural frequency, relative

Table 3: Comparison of results between fuzzy Gaussian controller, numerical FEM analysis, and experimental setup.

Relative first natural frequency "fnf"	Relative second natural frequency "snf"	Relative third natural frequency "tnf"	Average relative first mode shape difference "fmd"	Average relative second mode shape difference "smd"	Average relative third mode shape difference "tmd"	Fuzzy Gaussian controller relative 1st crack depth "rcd1," 1st crack location "rcl1," 2nd crack depth "rcd2," 2nd crack location "rcl2"				FEM relative 1st crack depth "rcd1," 1st crack location "rcl1," 2nd crack depth "rcd2," 2nd crack location "rcl2"				Numerical relative 1st crack depth "rcd1," 1st crack location "rcl1," 2nd crack depth "rcd2," 2nd crack location "rcl2"				Experimental relative 1st crack depth "rcd1," 1st crack location "rcl1," 2nd crack depth "rcd2," 2nd crack location "rcl2"			
						rcd1	rcl1	rcd2	rcl2	rcd1	rcl1	rcd2	rcl2	rcd1	rcl1	rcd2	rcl2	rcd1	rcl1	rcd2	rcl2
0.9987	0.9993	0.9996	0.0092	0.0027	0.0036	0.163	0.123	0.24	0.373	0.163	0.123	0.24	0.373	0.160	0.120	0.21	0.37	0.169	0.128	0.27	0.377
0.9968	0.9996	0.9992	0.0002	0.9712	0.2259	0.331	0.123	0.415	0.49	0.330	0.121	0.414	0.48	0.327	0.119	0.409	0.48	0.336	0.129	0.420	0.52
0.9924	0.9986	0.9995	0.0149	0.01	0.0826	0.413	0.124	0.330	0.875	0.412	0.122	0.329	0.873	0.408	0.118	0.326	0.87	0.419	0.127	0.336	0.879
0.9983	0.9997	0.9986	0.002	0.0034	0.0809	0.164	0.25	0.25	0.5	0.162	0.23	0.24	0.49	0.158	0.23	0.24	0.48	0.169	0.29	0.27	0.53
0.9980	0.9964	0.9883	0.0023	0.0333	0.0132	0.25	0.25	0.414	0.76	0.24	0.24	0.413	0.74	0.22	0.23	0.41	0.73	0.29	0.29	0.418	0.79
0.9992	0.9977	0.9975	0.3721	0.3416	0.2614	0.415	0.25	0.165	0.51	0.414	0.24	0.163	0.49	0.411	0.23	0.159	0.47	0.419	0.28	0.170	0.54
0.9852	0.9985	0.9864	0.0149	0.0201	0.0122	0.50	0.25	0.25	0.73	0.48	0.23	0.25	0.74	0.47	0.24	0.25	0.74	0.53	0.29	0.28	0.77
0.9994	0.9965	0.9968	0.0012	0.0013	0.0082	0.165	0.374	0.24	0.623	0.163	0.373	0.24	0.622	0.159	0.37	0.22	0.621	0.171	0.379	0.29	0.627
0.9985	0.9850	0.9885	0.0064	0.0083	0.0287	0.332	0.374	0.49	0.624	0.331	0.374	0.49	0.623	0.329	0.373	0.49	0.620	0.338	0.379	0.53	0.628
0.9991	0.99641	0.9994	0.0049	0.0032	0.0148	0.414	0.374	0.25	0.625	0.413	0.373	0.24	0.624	0.411	0.37	0.23	0.623	0.419	0.378	0.28	0.629

third natural frequency, average relative first mode shape difference, average relative second mode shape difference, and average relative third mode shape difference. The outputs from the fuzzy controller are relative crack depth and relative crack location. Twenty numbers of the fuzzy rules out of several hundreds of fuzzy rules are being listed in Table 2. The fuzzy controller results when rule 6 and rule 19 are activated from Table 2 are shown in Figure 8.

5. Experimental Setup

Experiments are performed to determine the natural frequencies and mode shapes for different crack depths on Aluminum beam specimen ($800 \times 38 \times 6$ mm). The experimental setup is shown in Figure 9. The amplitude of transverse vibration at different locations along the length of the Aluminum beam is recorded by positioning the vibration pickup and tuning the vibration generator at the corresponding resonant frequencies. These results for first three modes are plotted in Figure 10. Corresponding numerical results are also presented in the same graph for comparison.

6. Discussion

The results from fuzzy controller and the information obtained from theoretical, finite element and experimental analysis of the cracked cantilever beam are depicted later.

Fuzzy logic systems promise an efficient way for damage assessment in a cracked structure. They are able to treat uncertain and imprecise information; they make use of knowledge in the form of linguistic rules. At first, the theoretical expressions for the cracked and uncracked beams are developed for calculation of natural frequencies, mode shapes following correct expression of strain energy release rate. From Figure 2, it is observed that the compliances increase with the increase in relative crack depth. Finite element analysis is being performed on the cracked beam element (Figure 5) to find out the vibration characteristics. The comparison between results obtained from theoretical analysis for cracked and uncracked beams with the magnified view at the vicinity of crack location is presented in Figure 4. Results from finite element analysis (FEA) and numerical analysis are compared for both uncracked and cracked beams and are shown in Figure 6. For validation of the information obtained from various methodologies for analysis of the cracked cantilever beam, an experimental setup is developed as shown in Figure 9. Experiments are performed on the Aluminum beam specimen ($800 \times 38 \times 6$ mm) to estimate the first three mode shapes which are compared with the mode shapes obtained from the analysis as mentioned earlier. The vibration signatures (natural frequencies, mode shapes) are used to establish the fuzzy rules for designing fuzzy controller based on Gaussian membership functions that are depicted in Figures 7(a) and 7(b). The linguistic terms of fuzzy rules in the present fuzzy controller are given in Table 1. Some of the actual rules made for the fuzzy controller of the present investigation are listed in Table 2. The outputs of the Gaussian fuzzy controller obtained by activating rule 6 and rule 19 from Table 2 are presented in Figure 8. The mode shapes obtained from experimental and numerical, finite element, fuzzy analysis for cracked and uncracked beams are compared graphically in Figure 10. Some of the predicted outputs of the developed fuzzy controller and corresponding numerical finite element, and experimental results are presented in Table 3. It is observed that the results of all analyses are in good agreement.

7. Conclusions

In the present section, results obtained from the different analyses have the following conclusions.

As clear cut deviation of the mode shapes, natural frequencies can be detected for the cracked and uncracked beams at the vicinity of crack location. The comparison of results derived from theoretical and finite element method (FEM) for the cracked structure shows a good agreement. The fuzzy controller developed with Gaussian membership functions is designed with the help of the vibration signatures obtained from numerical and finite element analyses.

The first three relative natural frequencies and the first three mode shapes in dimensionless forms are the input parameters to the fuzzy inference system. Relative crack location and relative crack depth are the outputs from the system. The comparison of results between experimental and fuzzy analyses shows a close agreement. From the comparison of results, it is observed that the developed fuzzy inference system can predict the relative crack location and relative crack depth in a faster and accurate way, thereby decreasing a considerable amount of computational time. The proposed method can be used as an online condition monitoring tool, and in the future, hybrid technique can be developed for a faster and more efficient way for fault detection in the domain of dynamic vibrating structure.

References

[1] J. Yang, Y. Chen, Y. Xiang, and X. L. Jia, "Free and forced vibration of cracked inhomogeneous beams under an axial force and a moving load," *Journal of Sound and Vibration*, vol. 312, no. 1-2, pp. 166–181, 2008.

[2] S. Orhan, "Analysis of free and forced vibration of a cracked cantilever beam," *NDT and E International*, vol. 40, no. 6, pp. 443–450, 2007.

[3] M. T. Vakil-Baghmisheh, M. Peimani, M. H. Sadeghi, and M. M. Ettefagh, "Crack detection in beam-like structures using genetic algorithms," *Applied Soft Computing Journal*, vol. 8, no. 2, pp. 1150–1160, 2008.

[4] P. N. Saavedra and L. A. Cuitio, "Crack detection and vibration behavior of cracked beams," *Computers and Structures*, vol. 79, no. 16, pp. 1451–1459, 2001.

[5] N. Bakhary, H. Hao, and A. J. Deeks, "Damage detection using artificial neural network with consideration of uncertainties," *Engineering Structures*, vol. 29, no. 11, pp. 2806–2815, 2007.

[6] M. I. Friswell, J. E. T. Penny, and S. D. Garvey, "A combined genetic and eigensensitivity algorithm for the location of damage in structures," *Computers and Structures*, vol. 69, no. 5, pp. 547–556, 1998.

[7] Q. Wang, "A comprehensive stability analysis of a cracked beam subjected to follower compression," *International Journal of Solids and Structures*, vol. 41, no. 18-19, pp. 4875–4888, 2004.

[8] T. G. Chondros, A. D. Dimarogonas, and J. Yao, "A continuous cracked beam vibration theory," *Journal of Sound and Vibration*, vol. 215, no. 1, pp. 17–34, 1998.

[9] N. T. Khiem and T. V. Lien, "A simplified method for natural frequency analysis of a multiple cracked beam," *Journal of Sound and Vibration*, vol. 245, no. 4, pp. 737–751, 2001.

[10] E. Cam, S. Orhan, and M. Lüy, "An analysis of cracked beam structure using impact echo method," *NDT and E International*, vol. 38, no. 5, pp. 368–373, 2005.

[11] D. Y. Zheng and N. J. Kessissoglou, "Free vibration analysis of a cracked beam by finite element method," *Journal of Sound and Vibration*, vol. 273, no. 3, pp. 457–475, 2004.

[12] H. Tada, P. C. Paris, and G. R. Irwin, *The Stress Analysis of Cracks Hand Book*, Del Research Corporation, Hellertown, Pa, USA, 1973.

[13] A. S. Sekhar and B. S. Prabhu, "Crack detection and vibration characteristics of cracked shafts," *Journal of Sound and Vibration*, vol. 157, no. 2, pp. 375–381, 1992.

[14] M. A. Hossain, A. A. M. Madkour, K. P. Dahal, and H. Yu, "Comparative performance of intelligent algorithms for system identification and control," *Journal of Intelligent Systems*, vol. 17, no. 4, pp. 313–329, 2008.

[15] A. Ranjbaran, S. Hashemi, and A. R. Ghaffarian, "A new approach for buckling and vibration analysis of cracked column," *International Journal of Engineering A*, vol. 21, no. 3, pp. 225–230, 2008.

[16] Y. E. Zhou and A. E. Biegalski, "Problem diagnosis and retrofit of lateral bracing system of a truss bridge," in *Proceedings of the 2008 Structures Congress-Structures Congress 2008: Crossing the Borders*, vol. 314, April 2008.

[17] P. M. Pawar, K. Venkatesulu Reddy, and R. Ganguli, "Damage detection in beams using spatial fourier analysis and neural networks," *Journal of Intelligent Material Systems and Structures*, vol. 18, no. 4, pp. 347–359, 2007.

[18] K. Wada, N. Hayano, and H. Oka, "Application of the fuzzy control method for level control of a hopper," *Advanced Powder Technology*, vol. 2, no. 3, pp. 163–172, 1991.

[19] D. R. Parhi, "Navigation of mobile robots using a fuzzy logic controller," *Journal of Intelligent and Robotic Systems*, vol. 42, no. 3, pp. 253–273, 2005.

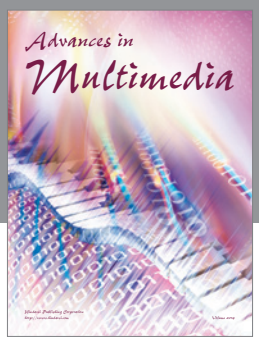

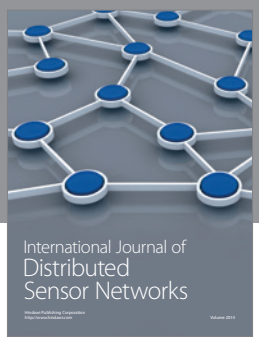

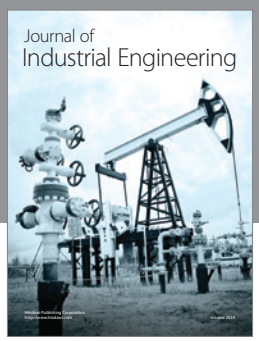

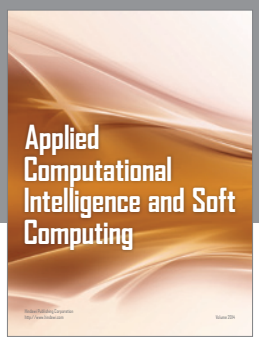

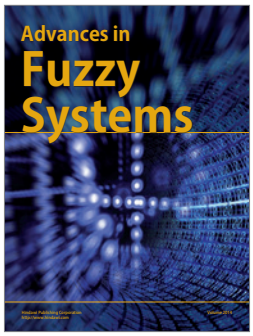

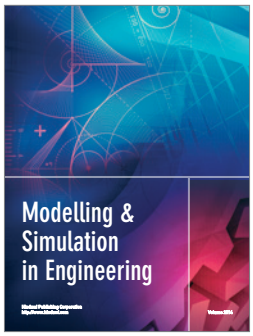

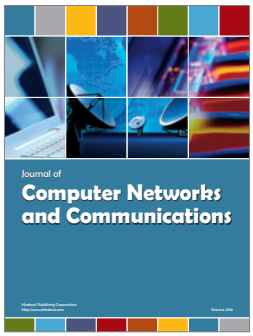

Hindawi

Submit your manuscripts at
http://www.hindawi.com